Evolution and Antigenic Drift of Influenza A(H7N9) Viruses, China, 2017–2019

Jiahao Zhang,[1] Hejia Ye,[1] Huanan Li,[1] Kaixiong Ma, Weihong Qiu, Yiqun Chen, Ziwen Qiu, Bo Li, Weixin Jia, Zhaoping Liang, Ming Liao, Wenbao Qi

After a sharp decrease of influenza A(H7N9) virus in China in 2018, highly pathogenic H7N9 viruses re-emerged in 2019. These H7N9 variants exhibited a new predominant subclade and had been cocirculating at a low level in eastern and northeastern China. Several immune escape mutations and antigenic drift were observed in H7N9 variants.

Since emerging in China in 2013, influenza A(H7N9) viruses have continued to circulate in mainland China, sporadically causing human infection (*1*–*3*). As of February 2020, a total of 1,568 laboratory-confirmed human cases and 616 related deaths had been reported, for a fatality rate of ≈40% (http://www.fao.org/ag/againfo/programmes/en/empres/H7N9/situation_update.html). In mid-2016, a highly pathogenic avian influenza (HPAI) virus of subtype H7N9 emerged, and the number of cases in humans began to rise sharply during a fifth wave (*4*,*5*). Animal studies indicated that these HPAI H7N9 viruses are highly virulent in chickens and have gained transmissibility among ferrets (*5*–*7*). Also, the cocirculation of HPAI (H7N9) viruses caused high genetic diversity and host adaption (*8*), posing public health concerns.

Although HPAI H7N9 viruses spread widely across China in 2017 (*8*,*9*), after an influenza H5/H7 bivalent vaccine for poultry was introduced in September 2017, the prevalence of the H7N9 viruses in birds and humans decreased dramatically (*6*,*10*). In early 2019, when the novel HPAI H7N9 viruses re-emerged, the isolation of HPAI H7N9 viruses from birds revealed them to be responsible for continuous epidemics in northeastern China (*11*). In March 2019, a human death in Gansu, China, was confirmed to have been caused by an H7N9 virus (*12*). To explore the prevalence and evolution of influenza A(H7N9) viruses, we sequenced 28 hemagglutinin (HA) and neuraminidase (NA) genes of poultry-origin H7N9 viruses circulating in China during 2019.

The Study

During January–December 2019, we conducted poultry surveillance for influenza virus at live poultry markets in 15 provinces of China (Appendix Figure 9, https://wwwnc.cdc.gov/EID/article/26/8/20-0244-App1.pdf). We isolated 28 H7N9 viruses from tracheal and cloacal swab samples of chickens in Shandong, Hebei, and Liaoning Provinces (Figure 1, panel C; Appendix Table 1). Vaccination of all chickens in China was compulsory according to the Ministry of Agriculture and Rural Affairs of the People's Republic of China. We sequenced the HA and NA genes of 28 H7N9 viruses and submitted the sequences to GISAID (https://www.gisaid.org) (Appendix Table 2). All H7N9 viruses had 4 continuous basic amino acids at cleavage sites (i.e., KRKRTAR/G and KRKRIAR/G), suggestive of high
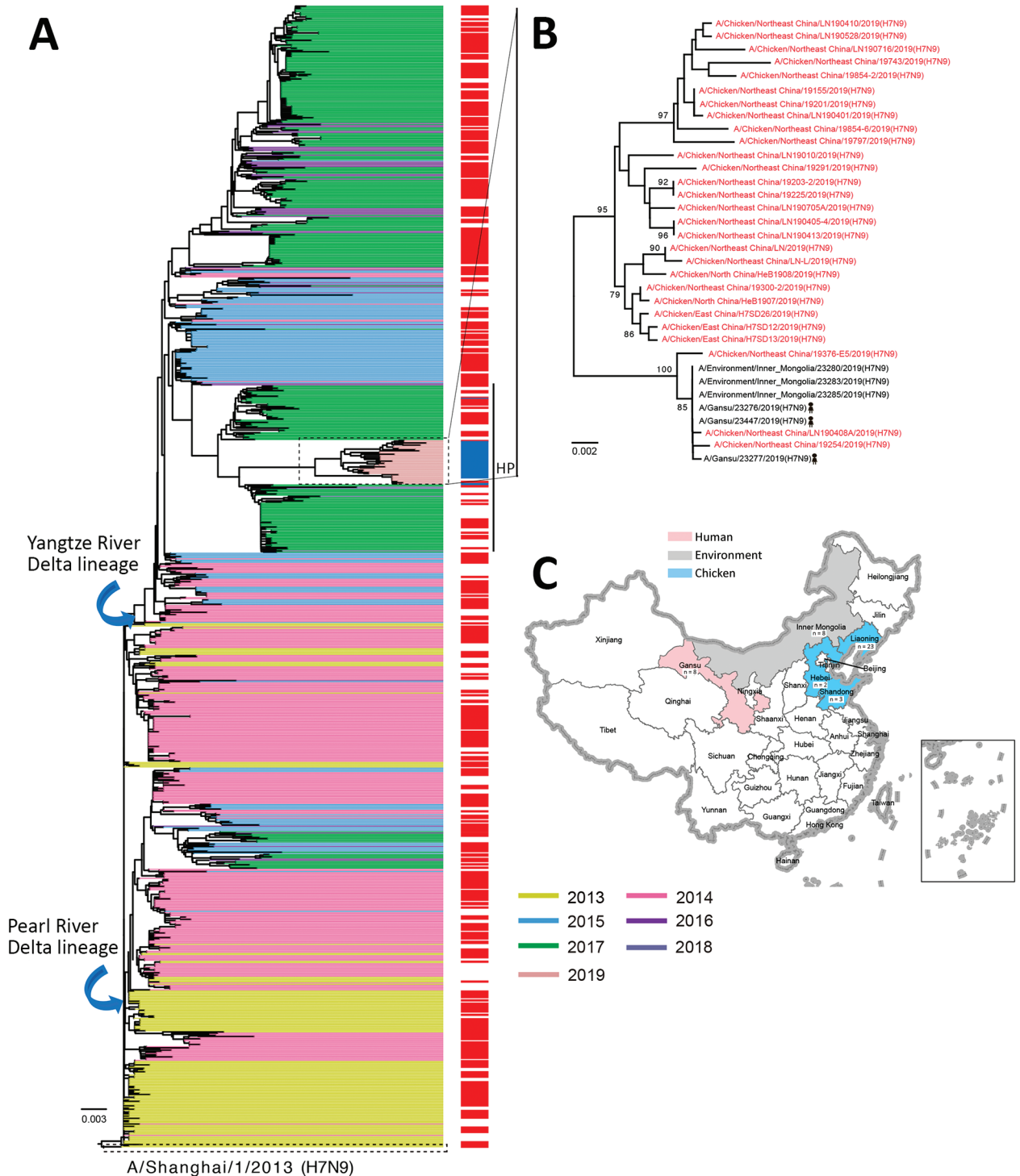
Author affiliations: College of Veterinary Medicine, South China Agricultural University, Guangzhou, China (J. Zhang, H. Li, K. Ma, Y. Chen, Z. Qiu, B. Li, W. Jia, M. Liao, W. Qi); National Avian Influenza Para-Reference Laboratory, Ministry of Agriculture and Rural Affairs of the People's Republic of China, Guangzhou (J. Zhang, H. Li, W. Jia, M. Liao, W. Qi); Key Laboratory of Animal Vaccine Development, Ministry of Agriculture and Rural Affairs of the People's Republic of China, Guangzhou (J. Zhang, W. Jia, M. Liao, W. Qi); National and Regional Joint Engineering Laboratory for Medicament of Zoonoses Prevention and Control, National Development and Reform Commission, Guangzhou (J. Zhang, W. Jia, M. Liao, W. Qi); Key Laboratory of Zoonoses Prevention and Control of Guangdong Province, Guangzhou (J. Zhang, W. Jia, M. Liao, W. Qi); Guangzhou South China Biological Medicine Co., Ltd, Guangzhou (H. Ye, W. Qiu, Z. Liang); Guangdong Laboratory for Lingnan Modern Agriculture, Guangzhou (W. Jia, M. Liao, W. Qi)

[1]These authors contributed equally to this article.

Figure 1. Evolutionary history of influenza A(H7N9) viruses, China, 2017–2019. A) Phylogenic tree of the hemagglutinin gene of H7N9 viruses. Colors indicate reference H7N9 viruses (n = 1,038) from each wave together with the H7N9 isolates from this study (panel B). Red on the right of the tree indicates isolates from humans. All branch lengths are scaled according to the numbers of substitutions per site. The tree was rooted by using A/Shanghai/1/2013(H7N9), which was collected in February 2013. B) Hemagglutinin gene tree revealing a single cluster of highly pathogenic H7N9 viruses circulating during 2019. Red indicates the H7N9 isolates from this study. Scale bar represents number of nucleotide substitutions per site. C) Distribution of highly pathogenic influenza A(H7N9) viruses during 2019. The backgrounds indicate the sampling spaces of highly pathogenic influenza A(H7N9) viruses during 2019 in humans (red), environment (gray), and chickens (blue). The map was designed by using ArcGIS Desktop 10.4 software (ESRI, http://www.esri.com).

pathogenicity. Phylogenic analysis demonstrated that the HA and NA genes of all of these HPAI H7N9 viruses belonged to the Yangtze River Delta lineage and formed a new subclade (Figure 1, panel A), which exhibited a long genetic distance to the HPAI H7N9 viruses that persisted during 2017–2018. In particular, the HA and NA genes of A/chicken/northeast China/19376-E5/2019(H7N9), A/chicken/northeast China/19254/2019(H7N9), and A/chicken/northeast China/LN190408A/2019(H7N9) were genetically closely related to the human-infecting influenza A(H7N9) viruses from Gansu (Figure 1, panel B; Appendix Figures 1–3), implying the potential risk for the reemerged HPAI H7N9 viruses to infect humans.

A root-to-tip regression analysis of temporal structure revealed aspects of the clock-like structure of 189 H7N9 viruses (correlation coefficient 0.89; R^2 0.95) during 2013–2019 (Figure 2, panel A). The epidemic HPAI H7N9 viruses had circulated in China since 2017 and can be classified into 2 sublineages, A and B. The HA and NA genes of the HPAI H7N9 viruses in 2019 belonged to a new sublineage B, whereas the HPAI H7N9 viruses circulating in 2017–2018 grouped into sublineage A (Figure 2, panel B; Appendix Figures 4, 5). Using the evolutionary rates of HA and NA, we estimated the times of origin (95% highest population density) of HPAI H7N9 viruses in sublineage B, which were September 2017–June 2018 for HA and April 2017–May 2018 for NA. Our HPAI H7N9 isolates exhibited traits of sublineages B-1 and B-2. We observed that the HPAI H7N9 viruses in eastern and northeastern China belonged to sublineage B-2 (Figure 2, panel B). However, in mid-2019, the HPAI H7N9 viruses continued to evolve and formed sublineage B-1, which suggested that the estimated times to the most recent common ancestors were May 2019 for HA genes and February 2019 for NA genes. Also, the human- and chicken-origin HPAI H7N9 viruses from Liaoning, Gansu, and Inner Mongolia clustered together in sublineage B-1. These results indicate that the poultry-origin H7N9 virus in sublineage B-1 emerged before the human spillover event in March 2019.

Although no substantial difference surfaced in the substitution rate of HA genes between H7N9 viruses during 2017–2018 and the viruses during 2019, the increased substitution rate occurred in the first and second codons of reemerged HPAI H7N9 viruses (Appendix Table 4). In a maximum clade credibility tree of the HA gene, 9 independently occurring mutations gave rise to the new sublineage-B circulating in 2019, including A9S, R22K, E71K, I78V, T116K, V125T, A151T, K301R, D439N (H7 numbering, https://www.fludb.org/brc/ha-Numbering.spg) (Figure 2, panel B), and only the V125T and A151T substitutions of the HA protein were reported as immune escape mutations (13). In addition, sublineage B-1 appeared to have acquired 3 parallel K184R, I499V, I520T (H7 numbering) mutations. The prevailing K184R substitutions of HPAI H7N9 viruses occurred during 2019. The K184R mutation was located in the antigenic site B and receptor binding region (Appendix Figure 6), suggesting that K184R was a potential mediator of viral antigenicity.

We used a hemagglutinin inhibition assay with an antigen of 15 H7N9 viruses circulating during 2017–2019, along with specific antiserum of 6 H7N9 viruses and 2 commonly used reassortant inactivated vaccines, H7N9-Re-2 and H7N9-rGD76, as controls. Antiserum from chickens vaccinated with H7N9-Re-2 strains showed high titers (9–10 log$_2$) and with H7N9-rGD76 strains showed low titers (4–8 log$_2$) to the HPAI H7N9 viruses circulating during 2018–2019 (Table 1). Moreover, the cross–hemagglutinin inhibition assay suggested statistically significant antigenic differences between the HPAI H7N9 viruses circulating during 2017 and during 2018–2019 (Table 2; Appendix Figure 7), indicative of antigenic drift of the reemerged HPAI H7N9 viruses. H7N9-Re-2 and H7N9-rGD76 inactivated vaccines have been widely used in chicken populations in mainland China since 2019 (14). Of note, we found that the virus shedding of chickens vaccinated with H7N9-Re-2 and H7N9-rGD76 against HPAI H7N9 viruses during 2019 ranged from 30% to 80% (Appendix Table 3); therefore, a timely update of H7N9 vaccine is needed.

Next, we evaluated the protective efficacy of the new candidate H7N9 inactivated vaccine (H71903)—that is, reverse genetic recombinant carrying HA and NA of A/chicken/east China/H7SD12/2019(H7N9) with internal genes of A/duck/Guangdong/D7/2007(H5N2)—in chickens against the challenge of 4 HPAI H7N9 viruses prevailing in sublineage B in 2019. All of the control chickens challenged with the H7N9 viruses died within 6 days of challenge (Appendix Figure 8). However, virus shedding was not detected from any of the vaccinated chickens challenged with H7N9 viruses (Appendix Table 3), indicating that the new candidate H7N9 vaccine could provide sound protection for chickens against challenge with these reemerged H7N9 variants.
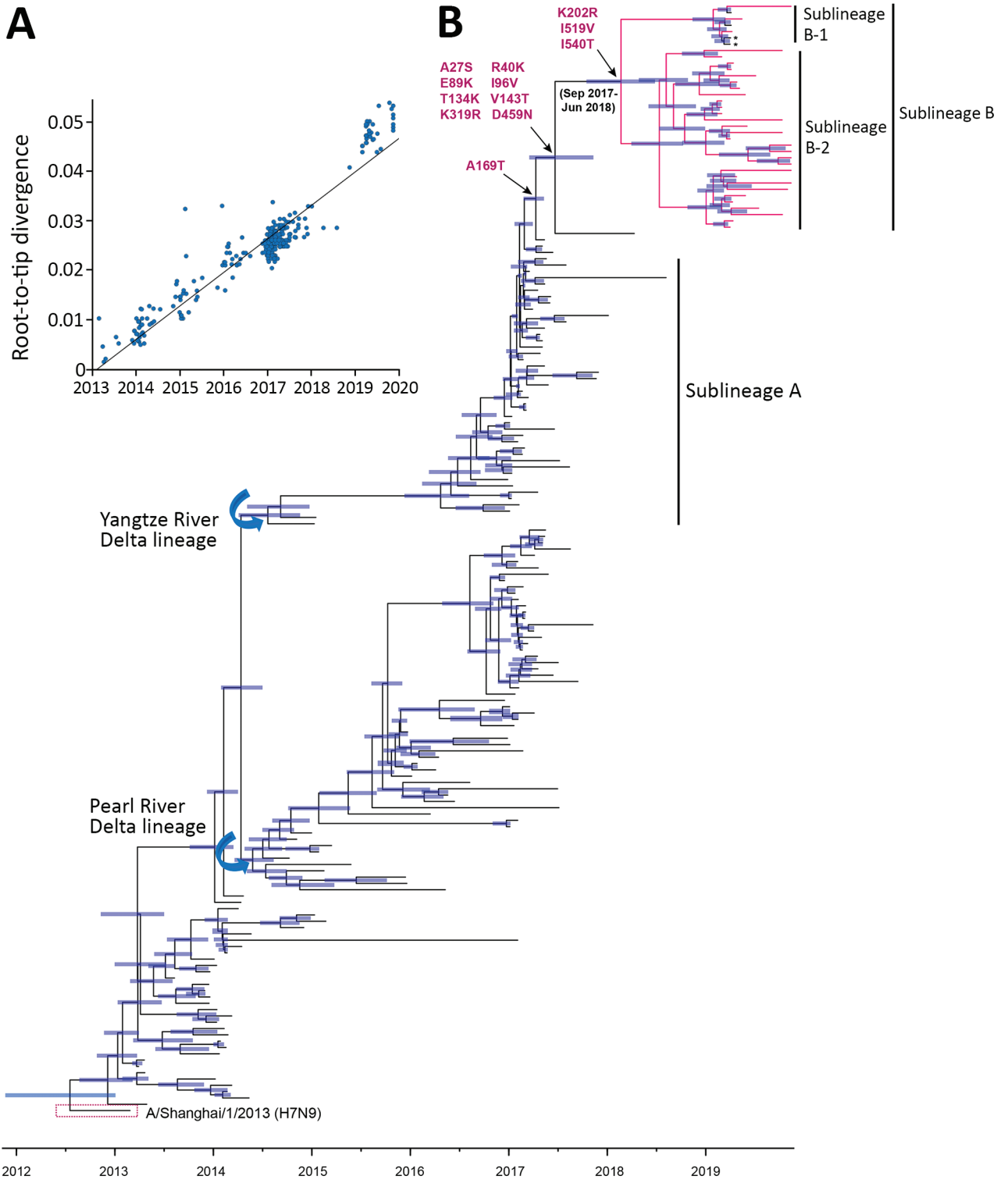
Figure 2. Time-scaled evolution of influenza A(H7N9) viruses, China. A) Analysis of root-to-tip divergence against sampling date for the hemagglutinin gene segment (n = 189). B) Maximum clade credibility tree of the hemagglutinin sequence of H7N9 viruses sampled in China (n = 189); the H7N9 viruses collected in this study are highlighted in red. Asterisk indicates viruses from a human with H7N9 infection within sublineage B during March 2019. Shaded bars represent the 95% highest probability distribution for the age of each node. Parallel amino acid changes along the trunk are indicated.

Table 1. Results of hemagglutinin inhibition assay in study of evolution and antigenic drift of influenza A(H7N9) viruses, China, 2019*

Antigen	Antiserum, titer							
	H7N9-Re-2†	H7N9-rGD76†	181115	H7SD12	H71903‡	LN19010	19225	19294
H7N9-Re-2	1,024	2,048	256	512	512	1,024	1,024	2,048
H7N9-rGD76	128	1,024	128	512	256	256	256	128
181115	64	256	1,024	256	256	256	128	128
H7SD12	64	256	256	1,024	1,024	2048	1,024	1,024
H71903	64	512	256	1,024	1,024	1,024	2048	1,024
LN19010	32	256	32	512	512	512	512	512
19225	32	256	64	1,024	512	1,024	512	1,024
19294	32	256	64	512	512	1,024	512	512
19300–1	32	256	64	1,024	512	1,024	512	512
19743	16	64	16	512	256	256	256	128
19797	16	32	16	256	128	128	64	128
19854–2	16	64	16	512	256	256	256	256
19854–6	16	64	16	256	256	512	256	256
LN191012	16	64	16	512	256	256	128	128
AH191005	32	128	32	1,024	512	256	256	256

*181115, A/chicken/northeast China/181115/2018(H7N9); H7SD12, A/chicken/east China/H7SD12/2019(H7N9); HeB1908, A/chicken/north China/HeB1908/2019(H7N9); LN19010, A/chicken/northeast China/LN19010/2019(H7N9); 19225, A/chicken/northeast China/19225/2019(H7N9); 19294, A/chicken/northeast China/19294/2019(H7N9); 19300–1, A/chicken/northeast China/19300–1/2019(H7N9); 19743, A/chicken/northeast China/19743/2019(H7N9); 19797, A/chicken/northeast China/197971/2019(H7N9); 19854–2, A/chicken/northeast China/19854–2/2019(H7N9); 19854–6, A/chicken/northeast China/19854–6/2019(H7N9); LN19010, A/chicken/northeast China/LN19010/2019(H7N9); LN191012, A/chicken/northeast China/LN191012/2019(H7N9); AH191005, A/chicken/east China/AH191005/2019(H7N9).
†H7N9-Re-2 and H7N9-rGD76 are vaccine strains widely used in China; both antigen and antiserum of H7N9-Re-2 were purchased from the Harbin Weike Biotechnology Development Company (www.hvriwk.com), the antigen of H7N9-Re-2 was available from reassortant avian influenza virus trivalent vaccine. The antigen and antiserum of H7N9-rGD76 were available from Guangzhou South China Biologic Medicine (http://www.gzscbm.com).
‡H71903 is candidate vaccine strain containing the hemagglutinin and neuraminidase genes from H7SD12 and 6 internal genes from A/duck/Guangdong/D7/2007(H5N2). H7SD12, 181115, HeB1908, LN19010, 19225, 19294, 19300–1, 19743, 19797, 19854–2, 19854–6, LN19010, LN191012, and AH191005 are highly pathogenic H7N9 strains in this study.

Conclusions

Our findings highlight that the HPAI H7N9 viruses that reemerged during 2019 had been cocirculating at a low level in eastern and northeastern China after the vaccination strategy was implemented. These HPAI H7N9 viruses continued to evolve and showed antigenic drift, posing a public health concern. Although vaccination can largely control the occurrence of H7N9 virus outbreaks, it can also accelerate the generation of novel variants. Therefore, comprehensive surveillance and enhancement of biosecurity precautions should be undertaken immediately to prevent the influenza virus epidemic from becoming a pandemic.

Table 2. r values of cross-hemagglutinin inhibition assay in study of evolution and antigenic drift of influenza A(H7N9) viruses, China, 2019*

Strain	Antiserum, r value							
	H7N9-Re-2	H7N9-rGD76	181115	H7SD12	H71903	LN19010	19225	19294
H7N9-Re-2	1	0.5	0.25	0.18	0.18	0.25	0.25	0.35
H7N9-rGD76	0.5	1	0.18	0.35	0.35	0.35	0.35	0.25
181115	0.25	0.18	1	0.25	0.25	0.13	0.13	0.13
H7SD12	0.18	0.35	0.25	1	1	1.41	1.41	1
H71903	0.18	0.35	0.25	1	1	1	1.41	1
LN19010	0.25	0.35	0.13	1.41	1	1	1.41	1.41
19225	0.25	0.35	0.13	1.41	1.41	1.41	1	1.41
19294	0.35	0.25	0.13	1	1	1.41	1.41	1

*H7N9-Re-2 and H7N9-rGD76 are vaccine strains widely used in China; both antigen and antiserum of H7N9-Re-2 were purchased from the Harbin Weike Biotechnology Development Company (http://www.hvriwk.com). The antigen of H7N9-Re-2 was available from reassortant avian influenza virus trivalent vaccine. The antigen and antiserum of H7N9-rGD76 were available from Guangzhou South China Biologic Medicine (http://www.gzscbm.com). H71903 is candidate vaccine strain containing the hemagglutinin and neuraminidase genes from H7SD12 and 6 internal genes from A/duck/Guangdong/D7/2007(H5N2). 181115, H7SD12, LN19010, 19225, and 19294 are highly pathogenic H7N9 strains in this study. r values indicate antigenic relatedness. r>1 indicates no significant antigenic difference between the strains; r = 1 indicates the same antigenicity; r<0.5 indicates a statistically significant antigenic difference between the strains. 181115, A/chicken/northeast China/181115/2018(H7N9); H7SD12, A/chicken/east China/H7SD12/2019(H7N9); LN19010, A/chicken/northeast China/LN19010/2019(H7N9); 19225, A/chicken/northeast China/19225/2019(H7N9); 19294, A/chicken/northeast China/19294/2019(H7N9).

About the Author

Dr. Zhang is a PhD student at South China Agricultural University, Guangzhou, China. His research interests are the epidemiology and pathogenesis of emerging and re-emerging infectious diseases.

References

1. Kang M, Lau EHY, Guan W, Yang Y, Song T, Cowling BJ, et al. Epidemiology of human infections with highly pathogenic avian influenza A(H7N9) virus in Guangdong, 2016 to 2017. Euro Surveill. 2017;22:22. https://doi.org/10.2807/1560-7917.ES.2017.22.27.30568
2. Wang X, Jiang H, Wu P, Uyeki TM, Feng L, Lai S, et al. Epidemiology of avian influenza A H7N9 virus in human beings across five epidemics in mainland China, 2013-17: an epidemiological study of laboratory-confirmed case series. Lancet Infect Dis. 2017;17:822–32. https://doi.org/10.1016/S1473-3099(17)30323-7
3. Liu D, Shi W, Shi Y, Wang D, Xiao H, Li W, et al. Origin and diversity of novel avian influenza A H7N9 viruses causing human infection: phylogenetic, structural, and coalescent analyses. Lancet. 2013;381:1926–32. https://doi.org/10.1016/S0140-6736(13)60938-1
4. Shi J, Deng G, Kong H, Gu C, Ma S, Yin X, et al. H7N9 virulent mutants detected in chickens in China pose an increased threat to humans. Cell Res. 2017;27:1409–21. https://doi.org/10.1038/cr.2017.129
5. Qi W, Jia W, Liu D, Li J, Bi Y, Xie S, et al. Emergence and adaptation of a novel highly pathogenic H7N9 influenza virus in birds and humans from a 2013 human-infecting low-pathogenic ancestor. J Virol. 2018;92:92.
6. Shi J, Deng G, Ma S, Zeng X, Yin X, Li M, et al. Rapid evolution of H7N9 highly pathogenic viruses that emerged in China in 2017. Cell Host Microbe. 2018;24:558–68. https://doi.org/10.1016/j.chom.2018.08.006
7. Bao L, Bi Y, Wong G, Qi W, Li F, Lv Q, et al. Diverse biological characteristics and varied virulence of H7N9 from wave 5. Emerg Microbes Infect. 2019;8:94–102. https://doi.org/10.1080/22221751.2018.1560234
8. Quan C, Shi W, Yang Y, Yang Y, Liu X, Xu W, et al. New threats from H7N9 influenza virus: spread and evolution of high- and low-pathogenicity variants with high genomic diversity in wave five. J Virol. 2018;92:92. https://doi.org/10.1128/JVI.00301-18
9. Lu J, Raghwani J, Pryce R, Bowden TA, Thézé J, Huang S, et al. Molecular evolution, diversity, and adaptation of influenza A(H7N9) viruses in China. Emerg Infect Dis. 2018;24:1795–805. https://doi.org/10.3201/eid2410.171063
10. Wu J, Ke C, Lau EHY, Song Y, Cheng KL, Zou L, et al. Influenza H5/H7 virus vaccination in poultry and reduction of zoonotic infections, Guangdong Province, China, 2017–18. Emerg Infect Dis. 2019;25:116–8. https://doi.org/10.3201/eid2501.181259
11. Jiang W, Hou G, Li J, Peng C, Wang S, Liu S, et al. Antigenic variant of highly pathogenic avian influenza A(H7N9) virus, China, 2019. Emerg Infect Dis. 2020;26:26. https://doi.org/10.3201/eid2602.191105
12. Yu D, Xiang G, Zhu W, Lei X, Li B, Meng Y, et al. The re-emergence of highly pathogenic avian influenza H7N9 viruses in humans in mainland China, 2019. Euro Surveill. 2019;24:13–21. https://doi.org/10.2807/1560-7917.ES.2019.24.21.1900273
13. Henry Dunand CJ, Leon PE, Huang M, Choi A, Chromikova V, Ho IY, et al. Both neutralizing and non-neutralizing human H7N9 influenza vaccine-induced monoclonal antibodies confer protection. Cell Host Microbe. 2016;19:800–13. https://doi.org/10.1016/j.chom.2016.05.014
14. Ministry of Agricultural and Rural Affairs of the People's Republic of China. No. 99 announcement [in Chinese] [cited 2018 Dec 13]. http://www.moa.gov.cn/gk/tzgg_1/gg/201812/t20181213_6164848.htm

Address for correspondence: Ming Liao and Wenbao Qi, No.483, Wushan Rd, Tianhe District, Guangzhou, Guangdong, China; email: mliao@scau.edu.cn and qiwenbao@scau.edu.cn

Evolution and Antigenic Drift of Influenza A(H7N9) Viruses, China, 2017–2019

Appendix

Methods

Ethics statement and biosafety

All experiments with all available influenza A(H7N9) viruses were conducted in an animal biosafety level 3 laboratory and animal facility under South China Agricultural University (SCAU) (CNAS BL0011) protocols. All animals involved in experiments were reviewed and approved by the Institution Animal Care and Use Committee at SCAU and treated in accordance with the guidelines (2017A002).

Sample collection and virus isolation

The cloacal and tracheal swab samples of chickens, ducks, and geese from live poultry markets were collected in 15 provinces of China, including Guangdong, Guangxi, Hebei, Shandong, Liaoning, Shaanxi, Hunan, Hubei, Sichuan, Jiangxi, Yunnan, Fujian, Henan, Chongqing, and Jilin provinces, during January–December 2019. Each sample was placed in 2 ml of the PBS supplemented with penicillin (5000 U/ml) and streptomycin (5000 U/ml). All the

samples were inoculated in the allantoic cavities of 10-day-old embryonated chicken egg at 37°C. The allantoic fluid was collected and tested for hemagglutinin (HA) assay with 1% chicken red blood cells and then used in this study.

RNA extraction, RT-PCR, and DNA sequencing

RNA was extracted from the suspension of virus isolates with the RNeasy Mini Kit (Qiagen) as directed by the manufacturer. Two-step RT-PCR was conducted with universal primers as previously described (*1*), and HA and neuraminidase (NA) gene segments were amplified under standard conditions (*1*). PCR products were purified with a QIAamp Gel extraction kit (Qiagen) and sequenced with an ABI 3730 DNA Analyzer (Applied Biosystems).

Phylogenic analysis

All the available HA and NA genomic sequences with the complete coding regions of influenza A(H7N9) viruses were downloaded from GenBank (http://ncbi.nlm.nih.gov/genbank/) and GISAID (http://www.gisaid.org/). The HA and NA sequences data set (sequences alignment was available on request) was then created. The downloaded HA and NA gene sequences together with new 28 H7N9 strains were aligned using the MAFFT (version 7.149) program (*2*). Maximum likelihood (ML) phylogenies for the codon alignment of the HA and NA gene segments were estimated using the GTRGAMMA nucleotide substitution model in the RAxML (version 8.2) program (*3*). Node support was determined by nonparametric bootstrapping with 1,000 replicates. The phylogenetic tree was visualized in the FigTree (version 1.4.3) program (http://tree.bio.ed.ac.uk/software/figtree/).

Bayesian maximum clade credibility (MCC) phylogeny of influenza A(H7N9) viruses

We estimated rates of evolutionary change (nucleotide substitution) in the HA and NA gene segments of the influenza A (H7N9) viruses. For efficiency of analysis we focused on the influenza A (H7N9) viruses sampled at different times and locations, which were representative of phylogenetic diversity of the influenza A (H7N9) viruses. To ensure that these had sufficient temporal structure in HA and NA alignment for reliable rate estimation, we first performed a regression of root-to-tip genetic distances on the ML tree against exact sampling dates using the TempEst (*4*). To obtain a more robust rate estimate, we used the Bayesian Markov chain Monte Carlo (MCMC) method implemented in the BEAST package (version 1.8.2), employing the GTR nucleotide substitution model, an uncorrected lognormal relaxed molecular clock model, and a Bayesian skyride coalescent model (*5*). Multiple runs of MCMC method were combined using LogCombiner (version 1.8.3), utilizing 1,500,000,000 total steps for each set, with sampling every 1,500 steps. Convergence (i.e., effective sample sizes > 200) of relevant parameters was assessed using Tracer (version 1.6) (http://beast.bio.ed.ac.uk/). The posterior distribution of trees obtained from BEAST analysis (with 10% of runs removed as burn-in) was also used to obtain the MCC tree for the HA and NA gene segments.

Structure-based mapping analysis

We predicted the HA monomer structure using the SWISS-Model website (https://swissmodel.expasy.org/), employing the A/Victoria/361/2011 (Protein Data Bank no.

4WE8) as a template. The amino acid corresponding to a three-dimensional (3D) amino acid

structure of the HA protein was mapped using MacPymol (http://www.pymol.org/).

Hemagglutinin inhibition (HI) and cross-hemagglutinin inhibition assays

HI assay was used to determine the HI titers (*1*). Antiserum from 21-day-old SPF

chickens challenged by five highly pathogenic avian influenza A(H7N9) viruses, including

A/Chicken/Northeast China/181115/2018(H7N9), A/Chicken/Northeast

China/H7SD12/2019(H7N9), A/Chicken/Northeast China/LN19010/2019(H7N9),

A/Chicken/Northeast China/19225/2019(H7N9), and A/Chicken/Northeast

China/19294/2019(H7N9), were prepared for HI assay. The antigens of 15 highly pathogenic

H7N9 strains during 2018–2019, as well as two commonly used vaccine strains, H7N9-Re-2 and

H7N9-rGD76, were used in this study. Both antigen and antiserum of H7N9-Re-2 were

purchased from the Harbin Weike Biotechnology Development Company, and the antigen and

antiserum of H7N9-rGD76 were available from Guangzhou South China Biological Medicine.

The HI test assay was a standard beta test, whereby 4 HA units of H7N9 viruses in 96-well plates

and the two-fold serially diluted serum prepared previously were added. The highest serum

dilution that produced complete inhibition of HA activity was regarded as HI endpoint titers.

Also, HI titers were used to calculate the antigenic relatedness (*r* values), calculated by the

Archetti and Horsfall (*6*) formulas: r_1 = HI titer of virus A antiserum vs virus B antigen/HI titer

of virus A antiserum vs virus A antigen; r_2 = HI titer of virus B antiserum vs virus A antigen/HI

titer of virus B antiserum vs virus B antigen: $r = \sqrt{r1 \times r2}$. $r > 1$ indicates no significant

antigenic difference between the strains, $r = 1$ indicates the same antigenicity, whereas $r < 0.5$ indicates a significant antigenic difference between the strains.

Plasmid construction and reverse genetics

The internal gene segments from the A/duck/Guangdong/D7/2007(H5N2) (D7) strain were cloned into the Hoffmann's bidirectional transcription vector pHW2000 plasmid system (*7*). The HA mutant (PEVPKGR/G cleavage site motif) of A/Chicken/East China/H7SD12/2019(H7N9) (H7SD12) was produced by site-directed mutagenesis PCR, and the NA gene of H7SD12 was also cloned into the pHW2000 plasmid system. The recombination H71903 carrying HA and NA genes of H7SD12 with internal gene segments D7 were generated using reverse genetics. Briefly, HEK293T cell monolayers in 6-well plates were transfected at 80–90% confluency with 4 μg of the eight plasmids (500 ng of each plasmid) using Lipofectamine 2000 (Invitrogen) according to the manufacturer's instructions. DNA and transfection reagent were mixed and incubated at room temperature for 5 min and added to the cells. Four hours later, the mixture was replaced with Opti-MEM (GIBCO) containing 0.2% bovine serum albumin and 1 μg/ml trypsin. After 48 hours, the supernatant was harvested and injected into SPF embryonated eggs for virus propagation. Viruses were titrated in embryonated eggs using HI assays, as recommended by the World Health Organization (WHO) manual on influenza diagnosis and surveillance. The H7N9 viruses were confirmed by RT-PCR and sequencing.

Vaccine test in chickens

The candidate H7N9 vaccine strain (H71903) contains the HA and NA genes from the H7SD12 and six internal genes from the D7. It is a formalin-inactivated oil-emulsion vaccine, with three parts inactivated allantonic fluid emulsified in two parts paraffin oil (volume/volume). To evaluate the protective efficiency of the candidate H71903 vaccine in chickens, groups of three-week-old SPF chickens (n=10) were inoculated intramuscularly with 0.3 ml of the vaccine or with an equal volume of PBS as a control. The concentration of vaccine strains should be $\geq$ 10^7 EID_{50} per 0.1 ml, and the HA titer should be no less than 1:256. Three weeks post-vaccination, serum was collected from the chickens for HI antibody testing. The chickens in each group were then challenged with 100 median lethal dose (LD_{50}) of the A/Chicken/East China/H7SD12/2019(H7N9), A/Chicken/East China/SD1115/2019(H7N9), A/Chicken/North China/HeB1908/2019(H7N9), and A/Chicken/Northeast China/LN/2019(H7N9) strains. Tracheal and cloacal swabs in 5 day post-infection were collected from all the surviving chickens and titrated in 10-day-old embryonated eggs. The chickens were observed for signs of diseases and death for two weeks.

Statistical analyses

Data are presented as mean $\pm$ standard deviation and were analyzed with GraphPad Prism 5.0. An independent samples t test was used for analysis.

References

<jrn>1. Qi W, Jia W, Liu D, Li J, Bi Y, Xie S, et al. Emergence and adaptation of a novel highly

pathogenic H7N9 influenza virus in birds and humans from a 2013 human-infecting low-

pathogenic ancestor. J Virol. 2018;92:92. PubMed</jrn>

<jrn>2. Katoh K, Misawa K, Kuma K, Miyata T. MAFFT: a novel method for rapid multiple sequence

alignment based on fast Fourier transform. Nucleic Acids Res. 2002;30:3059–66. PubMed

https://doi.org/10.1093/nar/gkf436</jrn>

<jrn>3. Stamatakis A. RAxML version 8: a tool for phylogenetic analysis and post-analysis of large

phylogenies. Bioinformatics. 2014;30:1312–3. PubMed

https://doi.org/10.1093/bioinformatics/btu033</jrn>

<jrn>4. Rambaut A, Lam TT, Max Carvalho L, Pybus OG. Exploring the temporal structure of

heterochronous sequences using TempEst (formerly Path-O-Gen). Virus Evol. 2016;2:vew007.

PubMed https://doi.org/10.1093/ve/vew007</jrn>

<jrn>5. Drummond AJ, Suchard MA, Xie D, Rambaut A. Bayesian phylogenetics with BEAUti and the

BEAST 1.7. Mol Biol Evol. 2012;29:1969–73. PubMed

https://doi.org/10.1093/molbev/mss075</jrn>

<jrn>6. Archetti I, Horsfall FL Jr. Persistent antigenic variation of influenza A viruses after incomplete

neutralization in ovo with heterologous immune serum. J Exp Med. 1950;92:441–62. PubMed

https://doi.org/10.1084/jem.92.5.441</jrn>

<jrn>7. Hoffmann E, Neumann G, Kawaoka Y, Hobom G, Webster RG. A DNA transfection system for generation of influenza A virus from eight plasmids. Proc Natl Acad Sci U S A. 2000;97:6108–13. PubMed https://doi.org/10.1073/pnas.100133697</jrn>

Appendix Table 1. Information on the influenza A(H7N9) viruses in this study

Name	Location	Host	Date	Subtype	Cleavage site sequence
A/Chicken/Northeast China/19155/2019(H7N9)	Liaoning	Chicken	2019/4/12	H7N9	KRKRTAR/G
A/Chicken/Northeast China/19201/2019(H7N9)	Liaoning	Chicken	2019/4/25	H7N9	KRKRTAR/G
A/Chicken/Northeast China/19203-2/2019(H7N9)	Liaoning	Chicken	2019/4/26	H7N9	KRKRTAR/G
A/Chicken/Northeast China/19225/2019(H7N9)	Liaoning	Chicken	2019/5/6	H7N9	KRKRTAR/G
A/Chicken/Northeast China/19254/2019(H7N9)	Liaoning	Chicken	2019/5/15	H7N9	KRKRTAR/G
A/Chicken/Northeast China/19291/2019(H7N9)	Liaoning	Chicken	2019/5/27	H7N9	KRKRTAR/G
A/Chicken/Northeast China/19300-2/2019(H7N9)	Liaoning	Chicken	2019/6/3	H7N9	KRKRTAR/G
A/Chicken/Northeast China/19743/2019(H7N9)	Liaoning	Chicken	2019/10/12	H7N9	KRKRTAR/G
A/Chicken/Northeast China/19797/2019(H7N9)	Liaoning	Chicken	2019/10/31	H7N9	KRKRTAR/G
A/Chicken/Northeast China/19854-2/2019(H7N9)	Liaoning	Chicken	2019/11/13	H7N9	KRKRTAR/G
A/Chicken/Northeast China/19854-6/2019(H7N9)	Liaoning	Chicken	2019/11/13	H7N9	KRKRTAR/G
A/Chicken/East China/H7SD12/2019(H7N9)	Shandong	Chicken	2019/3	H7N9	KRKRTAR/G
A/Chicken/East China/H7SD13/2019(H7N9)	Shandong	Chicken	2019/3	H7N9	KRKRTAR/G
A/Chicken/East China/H7SD26/2019(H7N9)	Shandong	Chicken	2019/3	H7N9	KRKRTAR/G
A/Chicken/Northeast China/LN19010/2019(H7N9)	Liaoning	Chicken	2019/3	H7N9	KRKRTAR/G
A/Chicken/Northeast China/LN-L/2019(H7N9)	Liaoning	Chicken	2019/4	H7N9	KRKRTAR/G
A/Chicken/Northeast China/LN190401/2019(H7N9)	Liaoning	Chicken	2019/4/1	H7N9	KRKRTAR/G
A/Chicken/Northeast China/LN190405-4/2019(H7N9)	Liaoning	Chicken	2019/4/5	H7N9	KRKRTAR/G

Name	Location	Host	Date	Subtype	Cleavage site sequence
A/Chicken/Northeast China/LN190408A/2019(H7N9)	Liaoning	Chicken	2019/4/8	H7N9	KRKRTAR/G
A/Chicken/Northeast China/LN190410/2019(H7N9)	Liaoning	Chicken	2019/4/10	H7N9	KRKRIAR/G
A/Chicken/Northeast China/LN190413/2019(H7N9)	Liaoning	Chicken	2019/4/13	H7N9	KRKRTAR/G
A/Chicken/Northeast China/LN190528/2019(H7N9)	Liaoning	Chicken	2019/5/28	H7N9	KRKRTAR/G
A/Chicken/Northeast China/LN190705A/2019(H7N9)	Liaoning	Chicken	2019/7/5	H7N9	KRKRTAR/G
A/Chicken/Northeast China/LN190716/2019(H7N9)	Liaoning	Chicken	2019/7/16	H7N9	KRKRTAR/G
A/Chicken/Northeast China/19376-E5/2019(H7N9)	Liaoning	Chicken	2019/4	H7N9	KRKRTAR/G
A/Chicken/North China/HeB1907/2019(H7N9)	Hebei	Chicken	2019/7	H7N9	KRKRTAR/G
A/Chicken/Northeast China/LN/2019(H7N9)	Liaoning	Chicken	2019/7	H7N9	KRKRTAR/G
A/Chicken/North China/HeB1908/2019(H7N9)	Hebei	Chicken	2019/8	H7N9	KRKRTAR/G

Appendix Table 2. The accession numbers in GISAID of the influenza A(H7N9) viruses in this study

| Name	ID sequence	HA accession #	NA accession #
A/Chicken/Northeast China/19155/2019(H7N9)	EPI_ISL_408420	EPI1679398	EPI1708369
A/Chicken/Northeast China/19201/2019(H7N9)	EPI_ISL_408421	EPI1679399	EPI1708368
A/Chicken/Northeast China/19203-2/2019(H7N9)	EPI_ISL_408422	EPI1679401	EPI1708367
A/Chicken/Northeast China/19225/2019(H7N9)	EPI_ISL_408423	EPI1679402	EPI1708366
A/Chicken/Northeast China/19254/2019(H7N9)	EPI_ISL_408424	EPI1679403	EPI1708364
A/Chicken/Northeast China/19291/2019(H7N9)	EPI_ISL_408425	EPI1679404	EPI1708365
A/Chicken/Northeast China/19300-2/2019(H7N9)	EPI_ISL_408426	EPI1679405	EPI1708363
A/Chicken/Northeast China/19743/2019(H7N9)	EPI_ISL_408419	EPI1679397	EPI1708370
A/Chicken/Northeast China/19797/2019(H7N9)	EPI_ISL_408427	EPI1679406	EPI1708362
A/Chicken/Northeast China/19854-2/2019(H7N9)	EPI_ISL_408428	EPI1679407	EPI1708361
A/Chicken/Northeast China/19854-6/2019(H7N9)	EPI_ISL_408429	EPI1679408	EPI1708359
A/Chicken/East China/H7SD12/2019(H7N9)	EPI_ISL_408432	EPI1679409	EPI1708330
A/Chicken/East China/H7SD13/2019(H7N9)	EPI_ISL_408433	EPI1679410	EPI1708329
A/Chicken/East China/H7SD26/2019(H7N9)	EPI_ISL_408434	EPI1679411	EPI1708328
A/Chicken/Northeast China/LN19010/2019(H7N9)	EPI_ISL_408435	EPI1679412	EPI1708327
A/Chicken/Northeast China/LN-L/2019(H7N9)	EPI_ISL_408436	EPI1679413	EPI1708325
A/Chicken/Northeast China/LN190401/2019(H7N9)	EPI_ISL_408437	EPI1679414	EPI1708326
A/Chicken/Northeast China/LN190405-4/2019(H7N9)	EPI_ISL_408438	EPI1679415	EPI1708324
A/Chicken/Northeast China/LN190408A/2019(H7N9)	EPI_ISL_408439	EPI1679416	EPI1708323
A/Chicken/Northeast China/LN190410/2019(H7N9)	EPI_ISL_408440	EPI1679417	EPI1708322
A/Chicken/Northeast China/LN190413/2019(H7N9)	EPI_ISL_408441	EPI1679418	EPI1708321
A/Chicken/Northeast China/LN190528/2019(H7N9)	EPI_ISL_408442	EPI1679419	EPI1708320
A/Chicken/Northeast China/LN190705A/2019(H7N9)	EPI_ISL_408443	EPI1679420	EPI1708318
A/Chicken/Northeast China/LN190716/2019(H7N9)	EPI_ISL_408444	EPI1679421	EPI1708317
A/Chicken/Northeast China/19376-E5/2019(H7N9)	EPI_ISL_408445	EPI1679422	EPI1708316
A/Chicken/North China/HeB1907/2019(H7N9)	EPI_ISL_408446	EPI1679423	EPI1708315
A/Chicken/Northeast China/LN/2019(H7N9)	EPI_ISL_408447	EPI1679424	EPI1708314
A/Chicken/North China/HeB1908/2019(H7N9)	EPI_ISL_408448	EPI1679425	EPI1708313

Appendix Table 3. Efficacy of H7N9 vaccines against highly pathogenic avian influenza A(H7N9) viruses, China, 2019

Vaccine	Challenge viruses	Mean HI titer 21 day after	
		vaccination	Trachea and Cloaca at 5 dpi
H7N9-Re-2	H7SD12	7.0±0.21	8/10
	SD1115	7.2±0.20	7/10
	HeB1908	7.6±0.16	7/10
	LN	7.5±0.17	6/10
H7N9-rGD76	H7SD12	7.2±0.20	3/10
	SD1115	7.1±0.18	4/10
	HeB1908	7.4±0.16	4/10
	LN	7.5±0.17	4/10
H71903	H7SD12	7.5±0.22	0/10
	SD1115	7.5±0.17	0/10
	HeB1908	7.1±0.23	0/10
	LN	7.5±0.17	0/10
Control	H7SD12	<1	10/10
	SD1115	<1	10/10
	HeB1908	<1	10/10
	LN	<1	10/10

Appendix Table 4. Nucleotide substitution rate of HA gene of influenza A(H7N9)

| Date	No. of isolates	Mean rate of nucleotide substitution (substitution/per/year)				
		Subs/site	95% HPD[*] (E^{-3})	1st	2nd	3rd
2017.1-2018.12	179	7.890E-3	[6.06, 9.93]	0.576	0.505	1.919
2019.1-2019.12	38	8.026E-3	[4.816, 11.40]	0.807	0.763	1.430

*HPD, highest probability density.
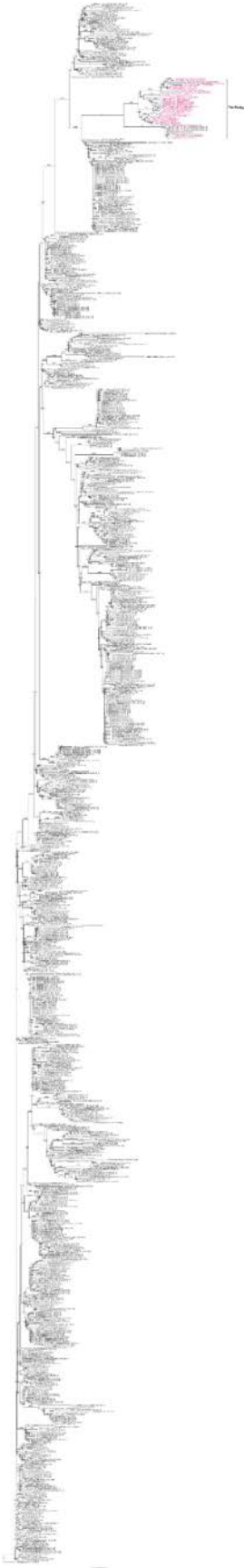
Appendix Figure 1. Phylogenic tree of H7N9 influenza viruses using HA gene sequences. The total HA genes (n=1038) of H7N9 viruses collected from 2013–2019 in China were analyzed. The tree is rooted to A/Shanghai/1/2013(H7N9). The red color indicates the H7N9 isolates in this study. The scale bar represents the number of nucleotide substitutions per site (subs/site).

Appendix Figure 2. Phylogenic tree of H7N9

viruses using NA gene sequences. The
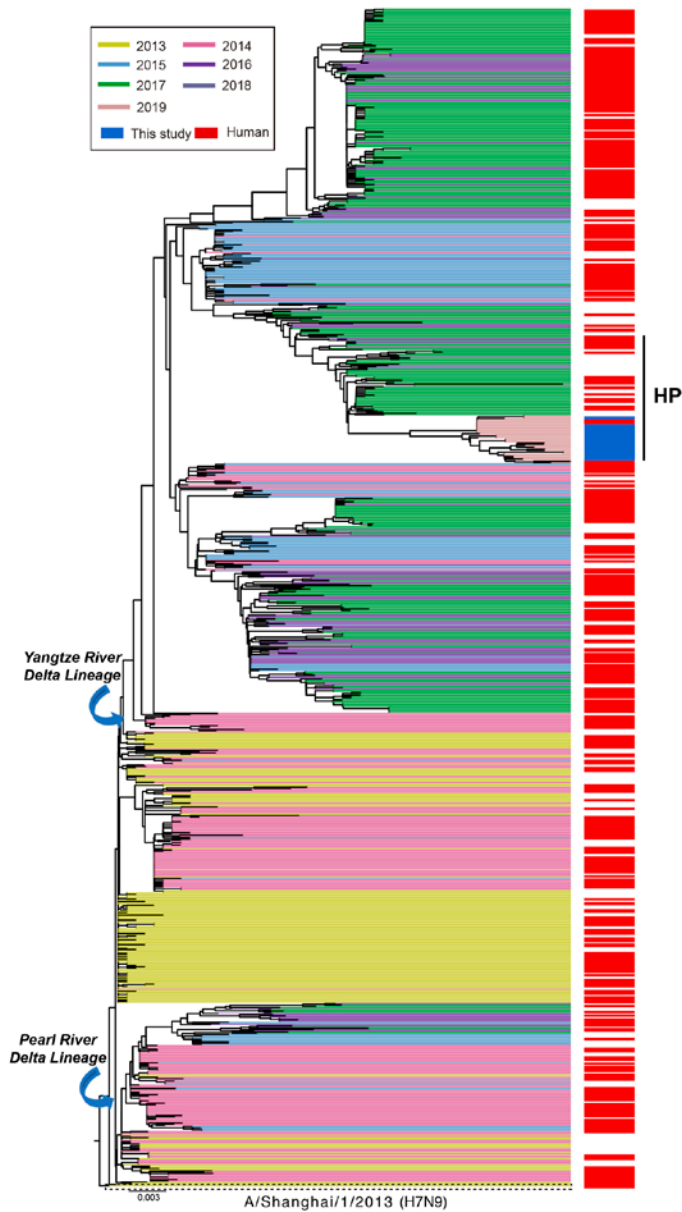
Appendix Figure 3. Phylogenic tree of the NA gene of H7N9 viruses. Reference H7N9 viruses from each

wave together with our H7N9 isolates (n=1014) were denoted by different colors. Red colors on the right

of the tree indicated the human isolates. All branch lengths were scaled according to the numbers of

substitutions per site (subs/site). The tree was rooted using A/Shanghai/1/2013(H7N9), which was

collected in February 2013.
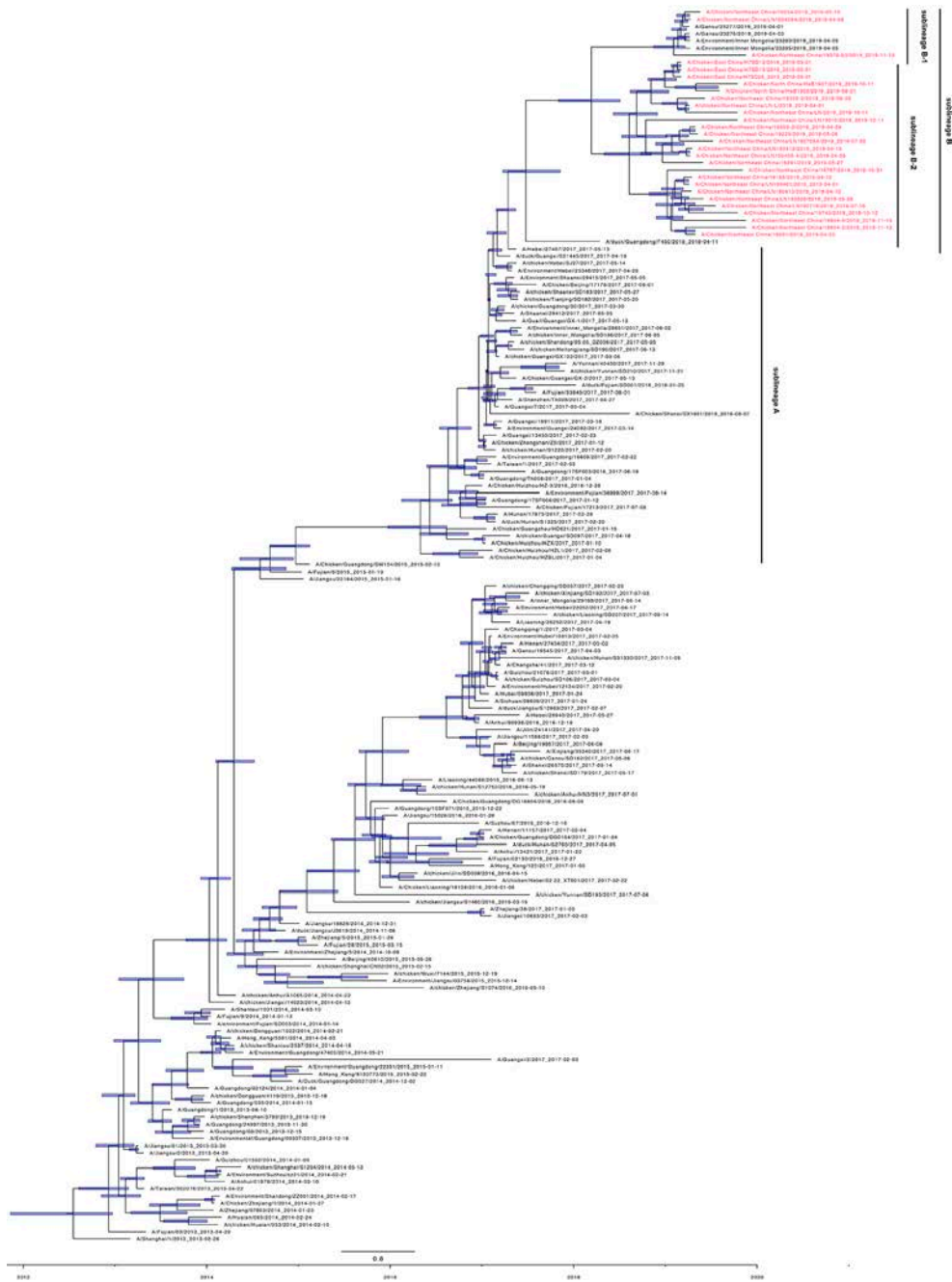
Appendix Figure 4. A maximum clade credibility tree of the HA sequence (n=189) of H7N9 viruses

sampled in China. The H7N9 viruses collected in this study highlighted in red. Shaded bars represent the

95% highest probability distribution for the age of each note.
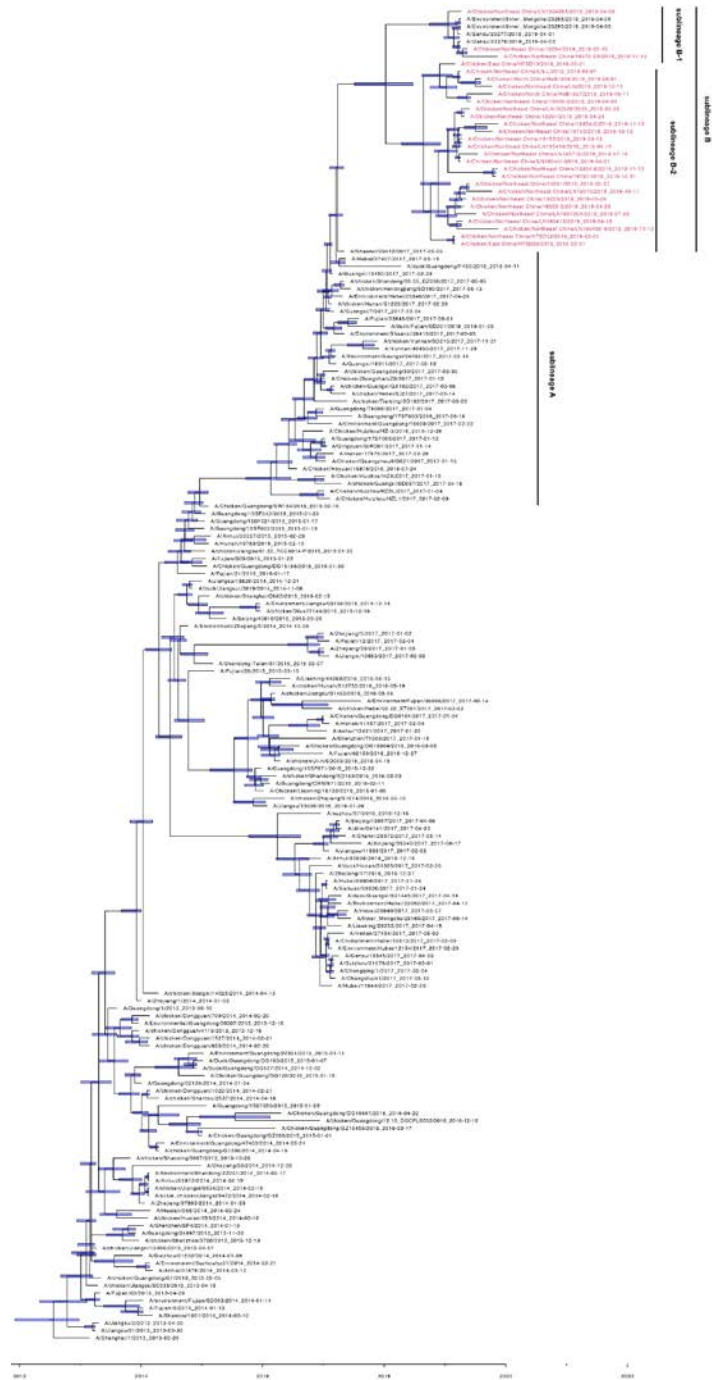
Appendix Figure 5. A maximum clade credibility tree of the NA sequence (n=178) of H7N9 viruses

sampled in China. The H7N9 viruses collected in this study highlighted in red. Shaded bars represent the

95% highest probability distribution for the age of each note.
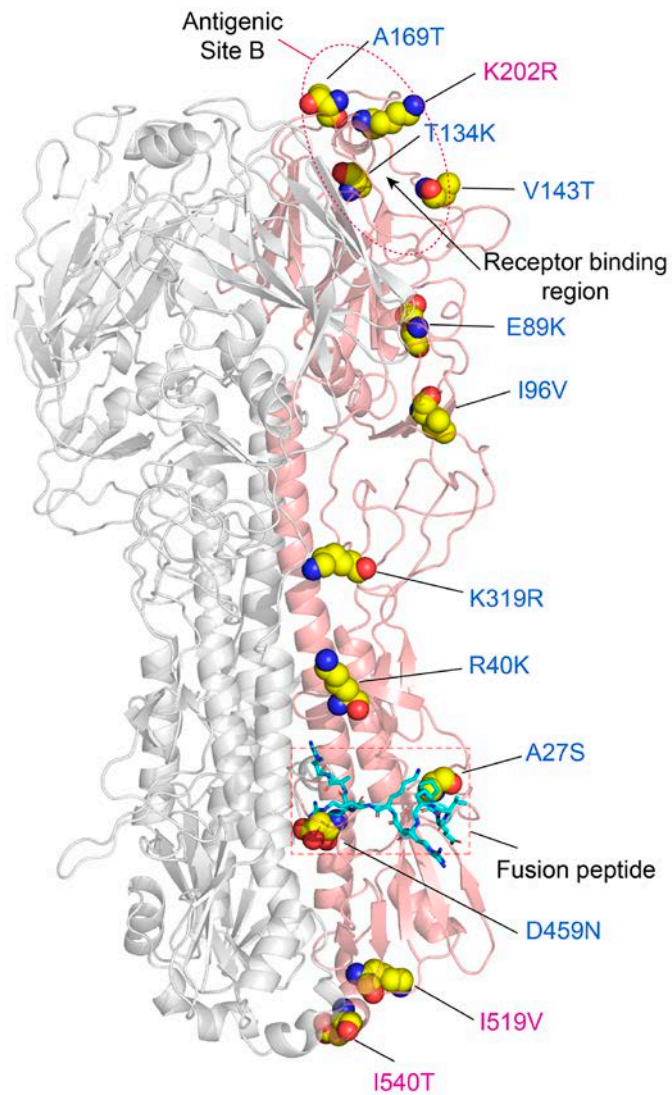
Appendix Figure 6. Structural analysis of amino acid changes of hemagglutinin in lineage B. The amino

acid substitutions are shown as spheres colored according to the constituent elements: carbon in yellow,

oxygen in red, and nitrogen in blue. The light blue indicates the putative fusion peptide. A side view of the

HA trimer structure of influenza virus based on A/Victoria/361/2011 (Protein Data Bank no. 4WE8) is

labeled as a template. The amino acids corresponding to the three-dimensional (3D) structure of the HA

protein were mapped using MacPymol (http://www.pymol.org/).
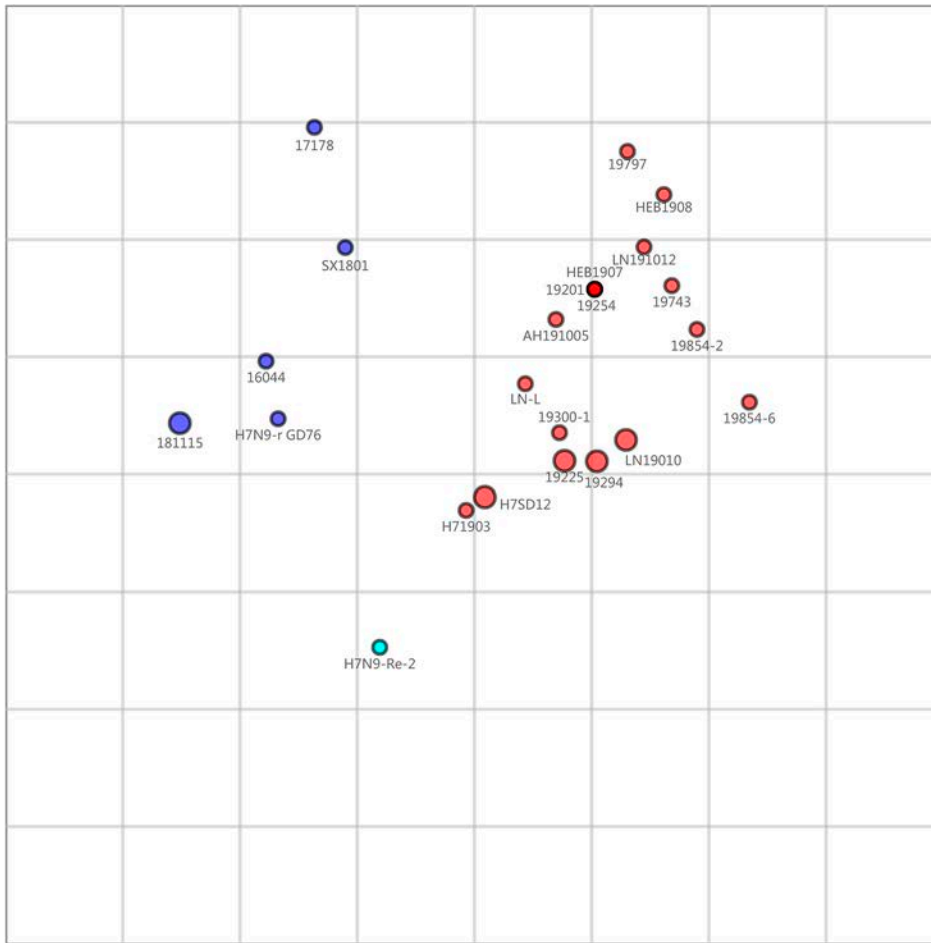
Appendix Figure 7. Antigenic map of influenza A(H7N9) viruses during 2017–2019 by cartography. The

hemagglutinin inhibition (HI) data were analyzed by using antigenic cartography (http://www.antigenic-

cartography.org), which is a method to visualize and increase the resolution of HI results. Each point on

the map represent an HA protein antigen. The distance between two HA protein antigens on the map

represents the antigenic distance between the two antigens. Points are colored based on categorical

hierarchical clustering.
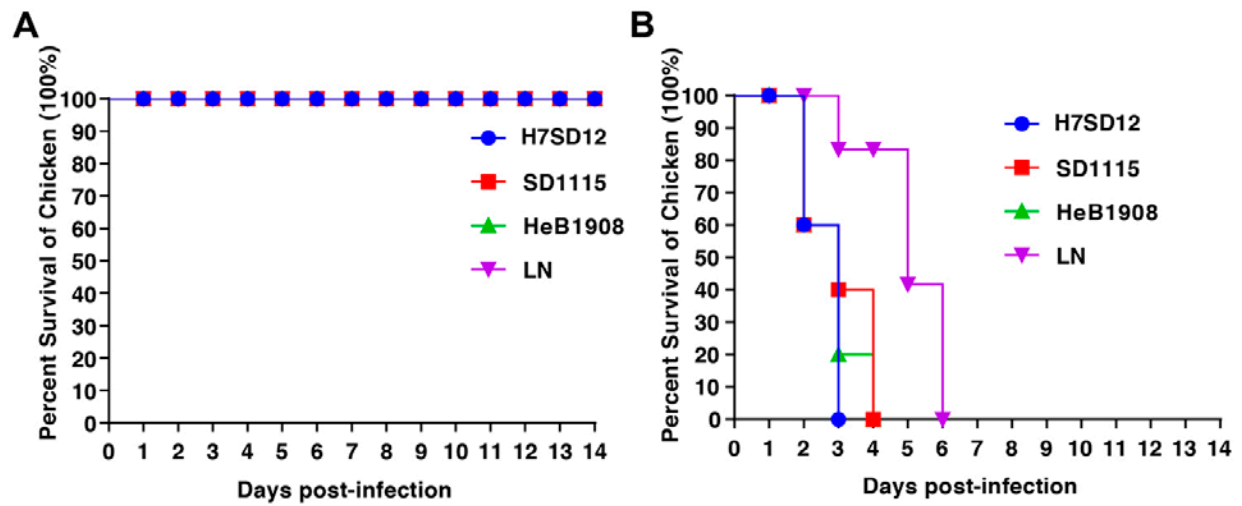
Appendix Figure 8. Protective efficacy of the candidate H71903 vaccine against challenge with four

H7N9 viruses in chickens. Survival rate of in vaccinated chickens (A) and non-vaccinated chickens (B)

challenged with four H7N9 viruses. H7SD12, A/Chicken/East China/H7SD12/2019(H7N9); SD1115,

A/Chicken/East China/SD1115/2019(H7N9); HeB1908, A/Chicken/North China/HeB1908/2019(H7N9);

LN, A/Chicken/Northeast China/LN/2019(H7N9).

Appendix Figure 9. Sample collection sites of poultry surveillance for avian influenza A viruses in mainland China, 2019. The gray background indicates the sample collection sites in this study.